Letters

Analytically Quantifying the Impact of Strength on Commutation Failure in Hybrid Multi-Infeed HVdc Systems

Hao Xiao, *Member, IEEE*, Xianzhong Duan, *Senior Member, IEEE*, Yi Zhang, *Fellow, IEEE*, Tongkun Lan, *Member, IEEE*, and Yinhong Li, *Senior Member, IEEE*

***Abstract*—The strength has a large impact on the commutation failure (CF) in hybrid multi-infeed HVdc (HMIDC) systems including both voltage-source converters and line-commutated converters. However, this impact has always been quantified by the simulation-based method in earlier works, which is very time-consuming and cannot lend the exhaustively theoretical perspective. Thus, in this letter, the mathematical expression of the CF immunity index as the analytical function of the hybrid multi-infeed interactive effective short-circuit ratio strength index is first developed based on the quasi-steady-state model of HMIDC systems. Thereafter, the developed expression is used for analytically quantifying the impact of the strength on the CF in a much more efficient manner with more sufficiently theoretical perspective compared to the simulation-based method in earlier works. Finally, the theoretical developments are validated by the experimental results of the hardware-in-the-loop platform based on a hybrid six-infeed HVdc test system.**

***Index Terms*—Commutation failure (CF), commutation failure immunity index (CFII), hybrid multi-infeed HVdc (HMIDC) systems, hybrid multi-infeed interactive effective short-circuit ratio (HMIESCR), strength.**

I. Introduction

RECENTLY, the increasing emergence of hybrid multi-infeed HVdc (HMIDC) systems, including both voltage-source converters (VSC) and line-commutated converters (LCC), has become a new development trend of modern ac/dc transmission networks [1]–[3]. One typical example of such systems is the China Guangdong Power Grid in 2020 with one VSC and nine LCC inverters incorporated into the common receiving end ac network [4]. In HMIDC systems, the commutation failure (CF) issue in LCC inverters under ac faults is a great threat to the system reliable operation [5]. Moreover, the CF is supposed to be largely impacted by the strength of HMIDC systems, since the latter depicts the voltage-support capability of the interconnected ac network to the concerned LCC inverter at the inverter bus [6]. Hence, quantifying the impact of the strength on the CF in HMIDC systems is very beneficial to the power industry.

In single-infeed LCC-HVdc systems including only single LCC inverter, the commutation voltage-time area theory has been utilized for predicting the critical inverter ac voltage depression indicative of the CF [7]. Based on this theory, it is well-recognized in the subsequent research that the effective short-circuit ratio (ESCR) strength index has an approximately linear impact on the CF by both the simulation-based and analytical methods [8]–[10]. Compared to single-infeed systems, it is more difficult to accurately predict the CF behaviors in multi-infeed LCC-HVdc systems due to the interactions among multiple LCC inverters terminating at the common receiving end ac network. With these interinverter interactions depicted by the multi-infeed interaction factor index, it has been found that an LCC inverter with a higher ac strength has a smaller CF risk area in the ac network where ac faults will induce the CF in that inverter [11]. Besides, the ESCR is further reported to affect the CF with a near linear relationship by the simulated analysis [12] and analytical derivation [13], respectively. Note here that the nature of the abovementioned interinverter interactions consists in that the dynamic response characteristics of the involved inverters are interacted. More precisely, these characteristics of the concerned inverter are obviously different with and without the presence of the adjacent inverters due to the propagation of the dynamics by the tie-line impedances between inverter buses under ac faults. Different from the abovementioned multi-infeed LCC-HVdc systems, more complicated interinverter interactions exist in HMIDC systems, since VSC and LCC inverters there have various operational characteristics under diversified dc control modes [14]. This is because

Manuscript received September 20, 2021; revised November 4, 2021; accepted November 21, 2021. Date of publication December 2, 2021; date of current version January 19, 2022. This work was supported in part by the National Natural Science Foundation of China under Grant 51907067. *(Corresponding author: Tongkun Lan.)*

Hao Xiao is with the Department of Electrical and Computer Engineering, University of Manitoba, Winnipeg, MB R3T 2N2, Canada (e-mail: xiaohao_hvdc@163.com).

Xianzhong Duan, Tongkun Lan, and Yinhong Li are with the State Key Laboratory of Advanced Electromagnetic Engineering and Technology, Hubei Electric Power Security and High Efficiency Key Laboratory, School of Electrical and Electronic Engineering, Huazhong University of Science and Technology, Wuhan 430074, China (e-mail: xzduan@hust.edu.cn; t.k.lan@usask.ca; liyinhong@hust.edu.cn).

Yi Zhang is with the RTDS Technologies Inc., Winnipeg, MB R3T 2E1, Canada (e-mail: yizhang@rtds.com).

Color versions of one or more figures in this article are available at https://doi.org/10.1109/TPEL.2021.3132101.

Digital Object Identifier 10.1109/TPEL.2021.3132101

the characteristics of the concerned inverter are impacted by the propagation of the dynamics from only the adjacent LCC inverters in multi-infeed LCC-HVdc systems, whereas affected from both adjacent VSC and LCC inverters in HMIDC systems. Consequently, these complicated interactions in HMIDC systems also make the CF characteristics of the concerned LCC inverters much more difficult to be analyzed.

Although some research efforts have been made to quantify the impact of the strength on the CF in HMIDC systems, there are certain limits in those research [5], [15]. In [5], the multi-infeed interactive ESCR (MIESCR) strength index has been utilized for evaluating the susceptibility of the LCC inverters to CF in the simplified four-machine system and planned China Guangdong Power Grid in 2030 by the electromagnetic transient simulations. In [15], the apparent increase in the short-circuit ratio strength index has been used for assessing the effect of the adjacent VSC inverters on the CF characteristics of the concerned LCC inverters by the simulation analysis. The abovementioned discussions clearly indicate that the simulation-based method has always been employed in the impact-quantification research of the related earlier works [5], [15]. Nevertheless, this simulation-based method undoubtedly requires onerous electromagnetic transient simulations to be implemented. It is inevitable that these simulations are very time-consuming and cannot lend the exhaustively theoretical perspective. Note also that for more large-scale HMIDC systems in the future with lots of VSC and LCC inverters further planned, the required simulation time is actually unacceptable for guiding the planning and operation departments of the practical power grid.

Facing the abovementioned issues encountered in earlier works [5], [15], there is hence a strong motivation to analytically quantify the impact of the strength on the CF in HMIDC systems. Along with this philosophy, the following contributions are made in this letter: This letter extends the preliminary work in [20] and first uses the CF immunity index (CFII) to quantitatively evaluate the immunity of the concerned LCC inverters to the CF as well as the hybrid MIESCR (HMIESCR) index to effectively delineate the strength of HMIDC systems. Also, the mathematical expression of the CFII as the analytical function of the HMIESCR, as shown in the subsequent (8), is rigorously developed based on the system quasi-steady-state model with the complicated interinverter interactions considered. Second, it is further shown that the developed mathematical expression in (8) can be utilized for analytically quantifying the impact of the strength on the CF by the proposed analytical quantification method in this letter. Compared to the simulation-based method in earlier works, the proposed method is much more efficient as the time-consuming electromagnetic transient simulations are not required any more. Besides, since the impact of the strength on the CF is analytically evaluated in a more direct manner by using (8), more sufficiently theoretical perspective can also be provided by the proposed method than the simulation-based method.

The rest of this letter is structured as follows. In Section II, the mathematical expression of the CFII as the analytical function of the HMIESCR is developed. In Section III, analytically quantifying the impact of the strength on the CF is conducted. Finally, Section IV concludes this letter.

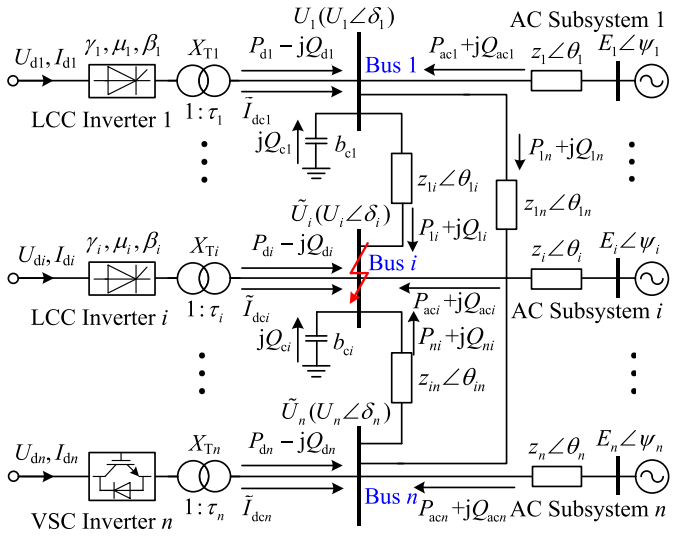

Fig. 1. Schematic diagram of the classical model of HMIDC systems including n inverters.

II. Developing the Mathematical Expression of the CFII as the Analytical Function of the HMIESCR

A. Classical Model of HMIDC Systems

The schematic diagram of the classical model of HMIDC systems including n VSC and LCC inverters is shown in Fig. 1. Therein, all ac subsystems for the CF investigation are represented by their Thevenin equivalent impedances and voltage sources. The electrical couplings among various inverters are physically reflected by the tie-line impedances between inverter buses. The presented system parameters and operation variables in Fig. 1 are expressed in per unit (p.u.) with the self-explanatory symbols. For all analysis hereafter related to Fig. 1, the rated active power of LCC inverter 1 (P_{d1N}) is selected as the base power, while the rated voltage of the common receiving end ac network (U_{N}) is used as the base voltage.

B. Developing the Mathematical Expression

Suppose that the three-phase line-to-ground fault happens at LCC inverter ac bus i ($i \in \{1, 2, \ldots, n\text{-}1, n\}$), as depicted by the red arrow in Fig. 1, with the corresponding fault inductance of L_{f}. Here, a lower L_{f} indicates a higher fault severity at LCC inverter ac bus i. In particular, when L_{f} decreases to the critical value $L_{\mathrm{f\_cri}}$, the CF will occur in LCC inverter i. Thus, $L_{\mathrm{f\_cri}}$ and also correspondingly critical fault impedance $Z_{\mathrm{f\_cri}} = \omega \cdot L_{\mathrm{f\_cri}}$ can be used to delineate the boundary of the CF in LCC inverter i, below which the CF is supposed to occur. For the further evaluation of the immunity of LCC inverter i to the CF with the abovementioned concepts, CFII_i has been specifically defined by CIGRE Working Group B4.41 as [6]

$$\mathrm{CFII}_i = \frac{U_{\mathrm{N}}^2 / Z_{\mathrm{f\_cri}}}{P_{\mathrm{d}i\mathrm{N}}} = \frac{U_{\mathrm{N}}^2 / (\omega \cdot L_{\mathrm{f\_cri}})}{P_{\mathrm{d}i\mathrm{N}}} \tag{1}$$

where $P_{\mathrm{d}i\mathrm{N}}$ denotes the rated active power of LCC inverter i.

Also, treat the fault with $L_{\mathrm{f\_cri}}$ at LCC inverter ac bus i as the critical external reactive power disturbance $\triangle Q_{i\_\mathrm{cri}} = \frac{U_{\mathrm{N}}^2/(\omega \cdot L_{\mathrm{f\_cri}})}{P_{\mathrm{d}i\mathrm{N}}}$ for inducing the CF in inverter i. Hence, $\triangle Q_{i\_\mathrm{cri}}$ and CFII_i in (1) have the same mathematical expression. Thereafter, CFII_i can be rewritten as

$$\mathrm{CFII}_i = \Delta Q_{i\_\mathrm{cri}} = \frac{\Delta Q_{i\_\mathrm{cri}}}{\Delta U_{i\_\mathrm{cri}}} \cdot \Delta U_{i\_\mathrm{cri}} \tag{2}$$

where $\triangle U_{i\_\mathrm{cri}}$ arising from $\triangle Q_{i\_\mathrm{cri}}$ is the critical value of the voltage depression at LCC inverter ac bus i ($\triangle U_i$) indicative of the boundary of the CF in LCC inverter i. If $\triangle U_i$ under the fault is larger than $\triangle U_{i\_\mathrm{cri}}$, the CF will occur. The expression of $\triangle U_{i\_\mathrm{cri}}$ can be obtained according to the LCC inverter quasi-steady-state model as [7], [11]

$$\Delta U_{i\_\mathrm{cri}} = U_i - \frac{X_{\mathrm{T}i}\tau_i I_{\mathrm{d}i}}{\cos\gamma_0 - \cos\beta_i}. \tag{3}$$

Here, $X_{\mathrm{T}i}$ and τ_i represent the converter transformer leakage reactance and turns ratio in LCC inverter i, $I_{\mathrm{d}i}$ and β_i denote the dc current and advance firing angle in LCC inverter i, respectively, and γ_0 is the minimum extinction angle for the successful commutation and is generally determined as 9° corresponding to the required 500 μs turn-OFF time of thyristors [7].

Note that $\triangle Q_{i\_\mathrm{cri}}$ and $\triangle U_{i\_\mathrm{cri}}$ in (2) are relatively small such that $\triangle Q_{i\_\mathrm{cri}}/\triangle U_{i\_\mathrm{cri}}$; there is actually the original definition of the voltage stability factor (VSF_i) at LCC inverter ac bus i indicative of the voltage stability of HMIDC systems in Fig. 1 [14]. Moreover, $\triangle Q_{i\_\mathrm{cri}}/\triangle U_{i\_\mathrm{cri}}$ can also be mathematically expressed in (6). Therein, Y_{ii} and Y_{ij} are, respectively, the magnitudes of the nodal self-admittance matrix element at LCC inverter ac bus i and mutual-admittance element between inverter ac buses j ($j \in \{1, 2, \ldots, n\text{-}1, n\}, j \neq i$) and i, $Q_{\mathrm{d}i}$ and $P_{\mathrm{d}i}$ are, respectively, the reactive and active powers in LCC inverter i, and $\partial Q_{\mathrm{d}i}/\partial U_i$ and $\partial P_{\mathrm{d}i}/\partial U_i$ are their corresponding reactive and active power–voltage dependence terms, respectively. It is further noted that the multi-infeed voltage interaction factor (MVIF_{ji}) index defined as the ratio of the magnitudes of the voltage vector changes at inverter ac buses j and i (i.e.,$|\Delta\tilde{U}_j|/|\Delta\tilde{U}_i|$) is used for the quantification of the interaction from inverter i to j in HMIDC systems [18].

Besides, to improve the accuracy of the strength evaluation, $\mathrm{HMIESCR}_i$ is proposed to delineate the strength of HMIDC systems referred at LCC inverter ac bus i [18]. For clarity, the detailed expression of $\mathrm{HMIESCR}_i$ is also given as

$$\mathrm{HMIESCR}_i = \frac{U_i^2(Y_{ii} - \sum_{j\neq i, j=1}^{n} Y_{ij} \cdot \mathrm{MVIF}_{ji})}{P_{\mathrm{d}i}}. \tag{4}$$

From which, it is known that

$$U_i^2(Y_{ii} - \sum_{j\neq i, j=1}^{n} Y_{ij} \cdot \mathrm{MVIF}_{ji}) = \mathrm{HMIESCR}_i \cdot P_{\mathrm{d}i}. \tag{5}$$

Substituting (5) into (6) further yields the detailed expression of $\triangle Q_{i\_\mathrm{cri}}/\triangle U_{i\_\mathrm{cri}}$ as the function of $\mathrm{HMIESCR}_i$ in (7). Thereafter, combining (2), (3), and (7), finally gives the mathematical expression of CFII_i as the analytical function of $\mathrm{HMIESCR}_i$ for HMIDC systems as shown in (8). It is worth mentioning that as the CF issue only occurs in LCC but not in VSC inverters under ac faults, the research focus has been put on the concerned LCC inverter i as the subject of this letter is the CF. However, no limitations of the types of the adjacent inverters in Fig. 1 are imposed when deriving (8) and the theoretical developments in this section are still valid even when other HVdc schemes are adopted in the adjacent inverters.

III. Analytically Quantifying the Impact of the Strength on the CF

A. Introduction of the Hybrid Six-Infeed HVdc Test System

The hybrid six-infeed HVdc test system (i.e., $n = 6$ in Fig. 1) is employed for validating the theoretical developments in Section II. In this test system, LCC inverters 1, 2, and 3 are terminated at ac buses 1, 2, and 3, respectively, while VSC inverters 4, 5, and 6 are located at ac buses 4, 5, and 6. To

$$\frac{\Delta Q_{i\_\mathrm{cri}}}{\Delta U_{i\_\mathrm{cri}}} = \mathrm{VSF}_i$$

$$= \frac{U_i^4(Y_{ii} - \sum_{j\neq i, j=1}^{n} Y_{ij} \cdot \mathrm{MVIF}_{ji})^2 - (Q_{\mathrm{d}i}^2 + P_{\mathrm{d}i}^2) + [U_i^2(Y_{ii} - \sum_{j\neq i, j=1}^{n} Y_{ij} \cdot \mathrm{MVIF}_{ji}) + Q_{\mathrm{d}i}]U_i\frac{\partial Q_{\mathrm{d}i}}{\partial U_i} + P_{\mathrm{d}i}U_i\frac{\partial P_{\mathrm{d}i}}{\partial U_i}}{[U_i^2(Y_{ii} - \sum_{j\neq i, j=1}^{n} Y_{ij} \cdot \mathrm{MVIF}_{ji}) + Q_{\mathrm{d}i}]U_i} \tag{6}$$

$$\frac{\Delta Q_{i\_\mathrm{cri}}}{\Delta U_{i\_\mathrm{cri}}} = \frac{(\mathrm{HMIESCR}_i \cdot P_{\mathrm{d}i})^2 - (Q_{\mathrm{d}i}^2 + P_{\mathrm{d}i}^2) + (\mathrm{HMIESCR}_i \cdot P_{\mathrm{d}i} + Q_{\mathrm{d}i})U_i\frac{\partial Q_{\mathrm{d}i}}{\partial U_i} + P_{\mathrm{d}i}U_i\frac{\partial P_{\mathrm{d}i}}{\partial U_i}}{(\mathrm{HMIESCR}_i \cdot P_{\mathrm{d}i} + Q_{\mathrm{d}i})U_i} \tag{7}$$

$$\mathrm{CFII}_i = \frac{(\mathrm{HMIESCR}_i \cdot P_{\mathrm{d}i})^2 - (Q_{\mathrm{d}i}^2 + P_{\mathrm{d}i}^2) + (\mathrm{HMIESCR}_i \cdot P_{\mathrm{d}i} + Q_{\mathrm{d}i})U_i\frac{\partial Q_{\mathrm{d}i}}{\partial U_i} + P_{\mathrm{d}i}U_i\frac{\partial P_{\mathrm{d}i}}{\partial U_i}}{(\mathrm{HMIESCR}_i \cdot P_{\mathrm{d}i} + Q_{\mathrm{d}i})U_i} \cdot \left(U_i - \frac{X_{\mathrm{T}i}\tau_i I_{\mathrm{d}i}}{\cos\gamma_0 - \cos\beta_i}\right)$$

$$= \frac{\mathrm{HMIESCR}_i^2 \cdot P_{\mathrm{d}i}^2 + \mathrm{HMIESCR}_i \cdot P_{\mathrm{d}i}U_i\frac{\partial Q_{\mathrm{d}i}}{\partial U_i} - (Q_{\mathrm{d}i}^2 + P_{\mathrm{d}i}^2) + Q_{\mathrm{d}i}U_i\frac{\partial Q_{\mathrm{d}i}}{\partial U_i} + P_{\mathrm{d}i}U_i\frac{\partial P_{\mathrm{d}i}}{\partial U_i}}{\mathrm{HMIESCR}_i \cdot P_{\mathrm{d}i} + Q_{\mathrm{d}i}} \cdot \left[1 - \frac{X_{\mathrm{T}i}\tau_i I_{\mathrm{d}i}}{U_i(\cos\gamma_0 - \cos\beta_i)}\right] \tag{8}$$

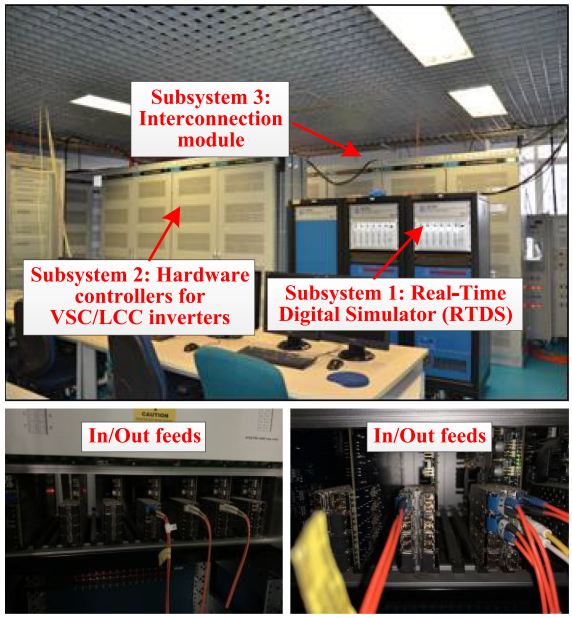

Fig. 2. Hardware-in-the-loop platform setup of the test system for the experimental verification.

take into account various dc control modes, the constant dc current/extinction angle control combination is used in LCC inverters 1 and 2, whereas the constant active power/extinction angle control combination is adopted in LCC inverter 3. Meanwhile, VSC inverters 4 and 5 operate at the constant active power/ac voltage control combination and VSC inverter 6 at the constant active power/reactive power control combination. Moreover, the system parameters and operation variables for LCC inverters are the same as the CIGRE HVdc benchmark model [16], [17]. Also, $z_1\angle\theta_1 = 0.1\angle 74.96°$ p.u., $z_2\angle\theta_2 = 0.3\angle 74.96°$ p.u., $z_3\angle\theta_3 = z_4\angle\theta_4 = z_5\angle\theta_5 = z_6\angle\theta_6 = 0.5\angle 74.96°$ p.u., $X_{\mathrm{T4}} = X_{\mathrm{T5}} = X_{\mathrm{T6}} = 0.15$ p.u., $\tau_4 = \tau_5 = \tau_6 = 1.0$ p.u., $P_{\mathrm{d4}} = P_{\mathrm{d5}} = P_{\mathrm{d6}} = 0.8$ p.u., $Q_{\mathrm{d4}} = Q_{\mathrm{d5}} = Q_{\mathrm{d6}} =$ -0.1 p.u., and the tie-line impedances between inverter buses are $1.0\angle 80.54°$ p.u.. Note that when system parameters values changed subsequently, they will be clarified in the related descriptions.

B. Description of the Hardware-in-the-Loop Platform

The hardware-in-the-loop platform setup of the abovementioned test system in Section III-A with the in/out-feeds is presented in Fig. 2 for the experimental verification under the real-time environment. For clarity, the corresponding architecture graph of the hardware-in-the-loop platform setup is also shown in Fig. 3. As can be seen there, the setup is primarily composed of three constituent subsystems. Subsystem 1 is the real-time digital simulator widely used in the power industry [18], in which the dc main circuits of the test system are modeled. Meanwhile, the expected functions of the involved VSC/LCC inverter controllers in Subsystem 2 are achieved with the use of the hardware. Moreover, the related signal exchange between Subsystems 1 and 2 is realized by the interconnection module including the analog-in and analog-out cards in Subsystem 3.

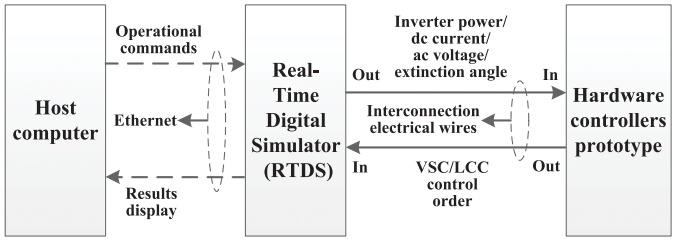

Fig. 3. Architecture graph of the hardware-in-the-loop platform setup.

More precisely, the signals transmitted from Subsystem 1 to 2 are the dc current, extinction angle, active power of LCC inverters as well as active power, ac voltage, and reactive power of VSC inverters. Accordingly, Subsystem 2 produces the VSC and LCC control orders in turn and outputs it to Subsystem 1.

C. Analytical Quantification and Experimental Validation

1) Analytical Quantification: In this section, the developed (8) is further utilized for analytically quantifying the impact of the strength on the CF in the abovementioned test system. For such purpose, consider both the 100-ms three-phase and single-phase faults occurring at $t = 1.2$ s at LCC inverter ac bus 1 under various z_1 in the preset range of interest from 0.10 to 0.70 p.u. with the steps of 0.05 p.u.. Note here that these classical fault test conditions have indeed been strongly recommended and approved in multiple CIGRE/IEEE standards and guides for the CF studies in LCC inverters. For example, two frequently referred ones are the CIGRE Guide "Systems With Multiple DC Infeed" [6] and IEEE Standard "IEEE Guide for Planning DC Links Terminating at AC Locations Having Low Short-Circuit Capacities" [19]. Besides, these fault conditions have already been widely applied in many related research papers on the CF analysis such as [5], [15], [16] [9]–[11]. With the abovementioned considerations, the theoretically calculated $\mathrm{HMIESCR}_1$ and CFII_1 for LCC inverter 1 by using (4) and (8), respectively, under various z_1 based on the MATLAB program are presented in Table I. Moreover, the three-phase and single-phase faults at LCC inverter ac buses 2 and 3 are also analyzed. Further, the theoretically calculated $\mathrm{HMIESCR}_2$ and CFII_2 for LCC inverter 2 under various z_2 as well as $\mathrm{HMIESCR}_3$ and CFII_3 for LCC inverter 3 under various z_3 are shown in Tables II and III, respectively. It is first seen in Table I that along with the reduced z_1, the calculated $\mathrm{HMIESCR}_1$ and CFII_1 both increase with an approximately linear relationship presented between them under both the three-phase and single-phase faults. A further inspection of Tables II and III also indicates the similar linear relationship between the calculated $\mathrm{HMIESCR}_2$ and CFII_2 as well as between the calculated $\mathrm{HMIESCR}_3$ and CFII_3. The abovementioned results therefore illustrate that the strength positively impacts the CF in a near linear manner when different fault types and points in the test system are comprehensively considered.

2) Experimental Validation: The experimental CFII_1, CFII_2, and CFII_3 acquired according to their definition in (1) under various z_1, z_2, and z_3, respectively, are further shown in Tables

TABLE I
ANALYTICALLY QUANTIFYING THE IMPACT OF $HMIESCR_1$ ON $CFII_1$ AND EXPERIMENTAL VALIDATION FOR BOTH THE THREE-PHASE AND SINGLE-PHASE FAULTS AT LCC INVERTER AC BUS 1 UNDER VARIOUS z_1 IN THE TEST SYSTEM

z_1 (pu)			0.10	0.15	0.20	0.25	0.30	0.35	0.40	0.45	0.50	0.55	0.60	0.65	0.70
$HMIESCR_1$		Cal.	12.850	9.518	7.852	6.852	6.186	5.711	5.354	5.077	4.856	4.675	4.524	4.396	4.287
$CFII_1$	Three-phase faults	Cal.	1.369	1.009	0.830	0.722	0.651	0.599	0.561	0.531	0.507	0.488	0.472	0.458	0.446
		Exp.	1.328	1.049	0.864	0.693	0.681	0.580	0.584	0.518	0.495	0.502	0.456	0.473	0.437
		Error	3.1 %	3.8 %	3.9 %	4.2 %	**4.4 %**	3.3 %	3.9 %	2.6 %	2.4 %	2.7 %	3.6 %	3.2 %	2.1 %

Notes: Cal.: Calculated. Exp.: Experimental. Error = |Cal. - Exp.| / Exp.

TABLE II
ANALYTICALLY QUANTIFYING THE IMPACT OF $HMIESCR_2$ ON $CFII_2$ AND EXPERIMENTAL VALIDATION FOR BOTH THE THREE-PHASE AND SINGLE-PHASE FAULTS AT LCC INVERTER AC BUS 2 UNDER VARIOUS z_2 IN THE TEST SYSTEM

z_2 (pu)			0.10	0.15	0.20	0.25	0.30	0.35	0.40	0.45	0.50	0.55	0.60	0.65	0.70
$HMIESCR_2$		Cal.	13.130	9.796	8.130	7.130	6.464	5.989	5.632	5.355	5.133	4.952	4.801	4.673	4.564
$CFII_2$	Three-phase faults	Cal.	1.399	1.039	0.860	0.752	0.680	0.629	0.591	0.561	0.537	0.518	0.502	0.488	0.476
		Exp.	1.349	1.069	0.886	0.736	0.664	0.605	0.617	0.542	0.553	0.500	0.488	0.498	0.461
		Error	3.7 %	2.8 %	2.9 %	2.2 %	2.4 %	3.9 %	**4.2 %**	3.6 %	2.9 %	3.5 %	2.8 %	2.0 %	3.3 %

Notes: Cal.: Calculated. Exp.: Experimental. Error = |Cal. - Exp.| / Exp.

TABLE III
ANALYTICALLY QUANTIFYING THE IMPACT OF $HMIESCR_3$ ON $CFII_3$ AND EXPERIMENTAL VALIDATION FOR BOTH THE THREE-PHASE AND SINGLE-PHASE FAULTS AT LCC INVERTER AC BUS 3 UNDER VARIOUS z_3 IN THE TEST SYSTEM

z_3 (pu)			0.10	0.15	0.20	0.25	0.30	0.35	0.40	0.45	0.50	0.55	0.60	0.65	0.70
$HMIESCR_3$		Cal.	13.230	9.893	8.226	7.227	6.561	6.085	5.728	5.451	5.229	5.048	4.897	4.769	4.660
$CFII_3$	Three-phase faults	Cal.	1.409	1.050	0.870	0.763	0.691	0.640	0.601	0.571	0.548	0.528	0.512	0.498	0.486
		Exp.	1.387	1.075	0.897	0.742	0.666	0.667	0.578	0.591	0.527	0.542	0.500	0.513	0.473
		Error	1.6 %	2.3 %	3.0 %	2.8 %	3.7 %	**4.1 %**	4.0 %	3.4 %	3.9 %	2.6 %	2.3 %	3.0 %	2.8 %

Notes: Cal.: Calculated. Exp.: Experimental. Error = |Cal. - Exp.| / Exp.

I, II, and III under both the three-phase and single-phase faults at LCC inverter ac buses 1, 2, and 3. Moreover, the detailed comparisons between the calculated and experimental $CFII_1$, $CFII_2$, and $CFII_3$ indicate that the maximum errors are 4.4%, 4.2%, and 4.1% as clearly marked by the bold font in those tables. These errors are deemed to be small enough for guiding the power industry. In other words, the developed (8) and consequently theoretical developments in Section II are validated by the experimental results of the test system under different fault types and points.

3) Comparison With the Simulation-Based Method in Earlier Works: The simulation-based method in earlier works [5], [15] is primarily realized with the electromagnetic transient simulations based on the PSCAD/EMTDC program. When the PSCAD/EMTDC program is running on an Intel i7 processor, 1.80 GHz, 32.0 GB RAM personal computer, it averagely takes about 100 min to obtain the simulated CFII in a single case for each selected z_1, z_2, or z_3 in Tables I–III. Thus, around 7800 min (130 h) for all 78 cases are required in total for the simulation-based method to get the simulated $CFII_1$, $CFII_2$, and $CFII_3$ with both the three-phase and single-phase faults at LCC inverter ac buses 1, 2, and 3 considered. On the contrary, only 2.1 s are totally required for all the theoretical calculations in the test system under different fault types and points in Tables I, II, and III using (8) by the proposed analytical quantification method in this letter. The abovementioned discussions therefore indicate that the proposed method is much more efficient than the simulation-based method, as the time-consuming electromagnetic transient simulations are not required any more. Besides, since the impact of the HMIESCR on the CFII is analytically evaluated in a more direct manner by using (8), more sufficiently theoretical perspective can also be provided by the proposed method than the simulation-based method.

IV. CONCLUSION

This letter first established the mathematical expression of the CFII as the analytical function of the HMIESCR based on the quasi-steady-state model of HMIDC systems. Then, the established expression was used for analytically quantifying the impact of the strength on the CF. This proposed analytical quantification method could be much more efficient and lend more sufficiently theoretical perspective when compared to the simulation-based method in earlier works. Finally, the validity of the theoretical developments was verified by the experimental results of a hybrid six-infeed HVdc test system.

REFERENCES

[1] Y. Xue, X. Zhang, and C. Yang, "Series capacitor compensated ac filterless flexible LCC HVDC with enhanced power transfer under unbalanced faults," *IEEE Trans. Power Syst.*, vol. 34, no. 4, pp. 3069–3080, Jul. 2019.
[2] W. Xiang, S. Yang, G. P. Adam, H. Zhang, W. Zuo, and J. Wen, "DC fault protection algorithms of MMC-HVDC grids: Fault analysis, methodologies, experimental validations, and future trends," *IEEE Trans. Power Electron.*, vol. 36, no. 10, pp. 11245–11264, Oct. 2021.

[3] F. Zhang, H. Xin, D. Wu, Z. Wang, and D. Gan, "Assessing strength of multi-infeed LCC-HVDC systems using generalized short-circuit ratio," *IEEE Trans. Power Syst.*, vol. 34, no. 1, pp. 467–480, Jan. 2019.

[4] B. Zhou *et al.*, "Principle and application of asynchronous operation of China Southern Power Grid," *IEEE J. Emerg. Sel. Topics Power Electron.*, vol. 6, no. 3, pp. 1032–1040, Sep. 2018.

[5] B. Cheng, Z. Xu, and W. Xu, "Optimal dc-segmentation for multi-infeed HVDC systems based on stability performance," *IEEE Trans. Power Syst.*, vol. 31, no. 3, pp. 2445–2454, May 2016.

[6] B. Davies, A. Williamson, A. M. Gole, B. EK, B. Long, and B. Burton *et al.*, "Systems with multiple DC infeed," CIGRE WG B4.41, Technical Brochure 364, Dec. 2008.

[7] C. V. Thio, J. B. Davies, and K. L. Kent, "Commutation failures in HVDC transmission systems," *IEEE Trans. Power Del.*, vol. 11, no. 2, pp. 946–957, Apr. 1996.

[8] X. Chen, A. M. Gole, and M. Han, "Analysis of mixed inverter/rectifier multi-infeed HVDC systems," *IEEE Trans. Power Del.*, vol. 27, no. 3, pp. 1565–1573, Jul. 2012.

[9] J. Wang, M. Huang, C. Fu, H. Li, S. Xu, and X. Li, "A new recovery strategy of HVDC system during AC faults," *IEEE Trans. Power Del.*, vol. 34, no. 2, pp. 486–495, Apr. 2019.

[10] L. Hong *et al.*, "Analysis and improvement of the multiple controller interaction in LCC-HVDC for mitigating repetitive commutation failure," *IEEE Trans. Power Del.*, vol. 36, no. 4, pp. 1982–1991, Aug. 2021.

[11] Y. Shao and Y. Tang, "Fast evaluation of commutation failure risk in multi-infeed HVDC systems," *IEEE Trans. Power Syst.*, vol. 33, no. 1, pp. 646–653, Jan. 2018.

[12] E. Rahimi, A. M. Gole, J. B. Davies, I. T. Fernando, and K. L. Kent, "Commutation failure analysis in multi-infeed HVDC systems," *IEEE Trans. Power Del.*, vol. 26, no. 1, pp. 378–384, Jan. 2011.

[13] H. Xiao, Y. Li, J. Zhu, and X. Duan, "Efficient approach to quantify commutation failure immunity levels in multi-infeed HVDC systems," *IET Gener. Transmiss. Distrib.*, vol. 10, no. 4, pp. 1032–1038, Mar. 2016.

[14] D. L. H. Aik and G. Andersson, "Analysis of voltage and power interactions in multi-infeed HVDC systems," *IEEE Trans. Power Del.*, vol. 28, no. 2, pp. 816–824, Apr. 2013.

[15] C. Guo, Y. Zhang, A. M. Gole, and C. Zhao, "Analysis of dual-infeed HVDC with LCC-HVDC and VSC-HVDC," *IEEE Trans. Power Del.*, vol. 27, no. 3, pp. 1529–1537, Jul. 2012.

[16] M. Szechtman, T. Wess, and C. V. Thio, "A benchmark model for HVDC system studies," in *Proc. Int. Conf. AC DC Power Transmiss.*, London, 1991, pp. 374–378.

[17] S. Mirsaeidi, D. Tzelepis, J. He, X. Dong, D. M. Said, and C. Booth, "A controllable thyristor-based commutation failure inhibitor for LCC-HVDC transmission systems," *IEEE Trans. Power Electron.*, vol. 36, no. 4, pp. 3781–3792, Apr. 2021.

[18] H. Xiao, X. Duan, Y. Zhang, and Y. Li, "Analytical evaluation approach of complex inter-inverter interactions in emerging hierarchical-infeed LCC-UHVDC systems," *IEEE Trans. Ind. Informat.*, early access, Oct. 14, 2021 doi: 10.1109/TII.2021.3119916

[19] *IEEE Guide for Planning DC Links Terminating at AC Locations Having Low Short-Circuit Capacities*, IEEE Standard 1204-1997, Jun. 1997.

[20] H. Xiao, Y. Li, and X. Duan, "Efficient approach for commutation failure immunity level assessment in hybrid multi-infeed HVDC systems," *J. Eng.*, vol. 2017, no. 13, pp. 719–723, Dec. 2017.